Available online at www.sciencedirect.com
SCIENCE DIRECT®
Chemical Physics Letters 391 (2004) 106–111
CHEMICAL PHYSICS LETTERS
www.elsevier.com/locate/cplett

Sensitive fluorescence spectroscopy of jet cooled $^{15}NO_2$

E.A. Volkers [a], A. Vredenborg [a], H. Linnartz [a,*], J. Bulthuis [a], S. Stolte [a], R. Jost [b]

[a] Department of Physical Chemistry, Laser Centre Vrije Universiteit, De Boelelaan 1083, NL-1081 HV Amsterdam, The Netherlands
[b] Laboratoire de Spectrométrie Physique, Université Joseph Fourier de Grenoble, B.P. 87, 38402 Saint Martin d'Hères Cedex, France

Received 19 February 2004; in final form 23 April 2004
Available online 18 May 2004

Abstract

A spectroscopic setup designed for high resolution spectroscopy of jet cooled molecules is described. The primary features of the new setup are an exceedingly low gas consumption and a high detection efficiency, which are achieved by optimizing the detection geometry of the time gated fluorescence in combination with a special piezo valve. This makes the setup particularly suitable for studying expensive gases that come in small supply. The performance of the setup is demonstrated on the first $A^2B_2 \leftarrow X^2A_1$ ro-vibronic transitions of $^{15}N^{16}O_2$ measured in a jet. A rotational analysis is given for a couple of different bands. In addition, an exceptionally strong band with band origin around 14 850 cm^{-1} is reported that is of interest particularly for atmospheric applications. The $^{15}N^{16}O_2$ gas consumption is as low as 0.025 mg or 0.5 μmol/cm^{-1} spectral range.

1. Introduction

In the last decade much progress has been achieved in recording and understanding the spectroscopic features of the atmospherically relevant NO_2 molecule (see [1–3] and references therein). The analysis of spectra in the near infrared and visible range of this triatomic molecule turned out to be difficult – even when the molecule is cooled in a jet expansion – because many spectral irregularities have been observed [1,4]. These are due to vibronic coupling between the X^2A_1 ground and the first electronically excited A^2B_2 state via the anti-symmetric stretch coordinate of b_2 symmetry and the appearance of a conical intersection between the two electronic states at a rather low energy of roughly 10 000 cm^{-1}. As a consequence only levels below and just above the conical intersection have been vibronically assigned. So far assignments of about 300 vibronic levels of $^{14}N^{16}O_2$ between zero and 12 000 cm^{-1} have been reported [1]. Most of these levels belong to the X^2A_1 ground state. For higher energies identifications are still ambiguous: above 16 500 cm^{-1} the nature of the spectra is essentially vibronically chaotic and one may expect that additional spectroscopic information from isotopic species with substantially different vibrational progressions will be interesting for a comparison. How, for instance, will the spectrum be affected in the asymmetrically substituted isotopologue, where the density of vibronic bright states is about twice that of the C_{2v} isotopologues? Also, a comparison of different isotopologues can be an important assignment tool: vibronic bands that show strong interactions between the lowest two diabatic electronic state in one isotopologue may well be nearly unperturbed in another one. Admittedly, this is only a realistic perspective in the spectral region just above the conical intersection, which we have not reached yet in our present measurements of $^{15}N^{16}O_2$.

Besides the pure fundamental interest in exploring the nuclear mass sensitivity of the non Born–Oppenheimer behaviour of the conical intersection, such a study is also of direct atmospheric relevance. A deviating isotope ratio of NO_2 molecules and NO_2 fragments may be due to a symmetry breaking as consequence of an isotope substitution. Such an anomalous isotopic distribution in the atmosphere, known as mass independent effect (MIF), has been observed for several atmospheric gases, e.g., nitrates, sulphates and particularly ozone [5–7] that has C_{2v} symmetry in its main isotopic composition ($^{16}O_3$). In recent work it was proposed that MIF can be

* Corresponding author. Fax: +31-20-4447643.
E-mail address: linnartz@chem.vu.nl (H. Linnartz).

0009-2614/$ - see front matter © 2004 Elsevier B.V. All rights reserved.
doi:10.1016/j.cplett.2004.04.077

explained by the symmetry breaking due to an isotope substitution that corresponds to C_s symmetry [8,9]. Very small differences in zero-point energies of the two exit channels for the dissociation of an asymmetric isotopomer, for example, are multiplied into substantial differences in the numbers of accessible states in the transition state. Similar effects are expected to take place upon isotope substitution in $^{x}O^{y}N^{z}O$ molecules. From an experimental point of view, however, high resolution jet studies of such isotopologues have been prohibitive so far because of large gas consumption. Previous jet studies use continuous expansion techniques with bolometer [10], cavity ring down [11] or (dispersed) fluorescence detection [12]. The pulsed jet experiments on $^{14}N^{16}O_2$ that have been reported, are photodissociation threshold [13] and nanosecond transient grating spectroscopy at sub-Doppler resolution [14]. The present study describes a time gated fluorescence experiment optimised for low gas consumption and high sensitivity.

From an analytical perspective it is relevant that in the present study of $^{15}N^{16}O_2$ we identified a very strong vibronic band around 14 850 cm^{-1}, which can be exploited for monitoring $^{15}N^{16}O_2$ in the atmosphere and for which a rotational analysis is presented.

2. Experiment

A schematic view of the experimental setup is shown in Fig. 1. Tuneable laser light with a bandwidth of approximately 0.07 cm^{-1} is generated using a dye laser that is pumped by the second harmonic of a Nd:YAG laser. A telescope is used to focus the laser beam into a vacuum setup. The vacuum setup consists of a large vacuum chamber differentially pumped by a 30 m^3/h rotary and a 1500 l/s diffusion pump, which is sufficient to keep the pressure below 10^{-4} mbar during beam operation. A high intensity piezo electric pulsed molecular beam source (nozzle diameter 0.7 mm) has been designed – based upon the model introduced by Proch and Trickl [15] – that is optimised for a well-defined pulse shape during a short opening time of about 150 μs.

A gas mixture of 1% $^{15}N^{16}O_2$ in Ar is used in all experiments. The $^{15}N^{16}O_2$ isotopologue is produced in a standard synthetic procedure from 99% pure $Na^{15}NO_3$ [16,17]. Sulphuric acid is added to sodiumnitrate–^{15}N to produce nitric acid. The mixture is distilled to obtain the nitric acid–^{15}N product. The $H^{15}NO_3$ reacts with P_2O_5 (phosphorus(V) oxide) to produce nitrogen (V) oxide–^{15}N. When heated to 260 °C $^{15}N_2O_5$ dissociates into $^{15}NO_2$ and O_2. The final separation is obtained in a cold trap that is operated at 213 K. The purity of the $^{15}N^{16}O_2$ obtained in this way is at least 95%, as has been checked with a mass spectrometer. The gas mixture is expanded with a backing pressure of 1.2 bar.

The laser beam crosses the expansion about 1.5 cm downstream. Spatial filtering and light baffles are used to improve the beam quality in the interaction zone. Two detectors are used to monitor the fluorescence zone. Downstream of the molecular beam (Fig. 1) a photomultiplier tube (PMT) sensitive in the 300–850 nm range is mounted. The PMT is gated to prevent saturation by direct scattered light of the laser beam. Perpendicular to the molecular beam a LN_2 cooled Ge detector (North Coast EO-817L) is mounted that is sensitive from 800 nm to 1.7 μm. An optical system is used to focus the fluorescence zone onto the active part of the detectors.

The timing sequence of the experiment is initiated by the Q-switch of the Nd:YAG laser. This signal is used to set the boxcar gates for the signal, calibration and power channels. A separate (and independent) pulse generator is used to control the Nd:YAG laser and the piezo valve. The gated signal of the PMT or Ge detector and the calibration signal are read by a computer and averaged over 10 laser pulses. The PC also controls the scan

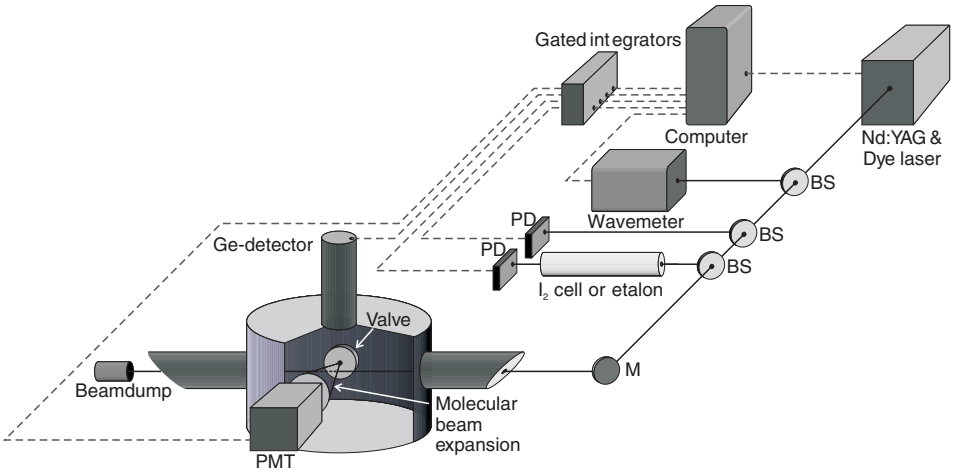

Fig. 1. A scheme of the experimental setup. Details are listed in the text (M, mirror; BS, beam splitter; PD, photo-detector).

procedure. The calibration signal is obtained by simultaneously recording an iodine absorption spectrum or the output of a wavemeter. An etalon (1.22 cm^{-1} FSR) signal is recorded to correct for possible deviations due to non-linear scanning of the dye laser. The latter is important, as the setup has been designed for fully automatic scanning over large frequency ranges, as large as 150 cm^{-1}. This gives an absolute accuracy in frequency better than 0.05 cm^{-1}.

3. Results and discussion

An overview scan of the $A^2B_2 \leftarrow X^2A_1$ of $^{15}N^{16}O_2$ is shown in Fig. 2 that covers part of the frequency range that has been studied up to now (13 800–18 000 cm^{-1}). Very strong bands belonging to the $^{14}N^{16}O_2$ isotopologue [12,18] are barely detectable, showing that the ^{15}N enrichment is nearly complete. About 300 vibronic bands have been measured for $^{15}N^{16}O_2$ with good S/N ratios.

With a repetition rate of 10 Hz about 3 mg $^{15}N^{16}O_2$ per hour is used. A typical 150 cm^{-1} long scan takes about an hour. This means that the absolute minimum gas amount that is necessary to cover the 13 800–18 000 cm^{-1} range amounts to less than 100 mg. During routine operation more gas is needed, typically between 300 and 500 mg, because of optimization tests, overlap between subsequent scans and repetition of scans to guarantee reproducibility. With cw jet and cw detection techniques such experiments are not affordable. The present setup, on the contrary, has the ability to cover large frequency regimes at high spectral resolution at exceedingly low gas consumption to study rare and expensive species. The focus in this paper will be on $^{15}N^{16}O_2$.

To illustrate the spectroscopic performance of our new setup, three zoomed and rotationally assigned bands are shown in Figs. 3–5.

A band with origin at 15 521 cm^{-1} is shown in Fig. 3. The rotational progression of a $K = 0$ parallel sub-band with each second rotational line missing can be seen: only transitions starting from even N levels (A_1 symmetry) are allowed. In contrast, even and odd N are allowed for the weaker $K = 1$ sub-band. The Q-branch of the $K = 1$ stack is observed close to the band origin of the $K = 0$ stack, indicating that the difference of the A rotational constant in ground and excited state is small. The 'staggering' effect observed in the $K = 1$ sub-band, i.e., the irregular spacings in the P and R-branches, is due to the slight deviation of NO_2 from a symmetric top. This enables us to determine the difference $B' - C'$ with good precision.

The parameters obtained from a non-linear least squares fit of this spectral region are given in Table 1. All spectral features are fitted, i.e., line intensities (both the rotational profiles and the intensity ratio of the $K = 0$ and 1 stack correspond to a rotational temperature of $T_{rot} = 8.5(1.5)$ K), line shapes (assuming Voigt profiles) and line positions. The good quality of the fit demonstrates that rovibronic couplings do not play an important role in this band, although especially the R_4 and R_5 transitions of the $K = 1$ stack are not reproduced that well. Also, fine structure splittings are negligible in this band, and therefore need not be included in the fit. Possible shifts induced by hyperfine couplings, notably the Fermi contact-coupling in the ground state,

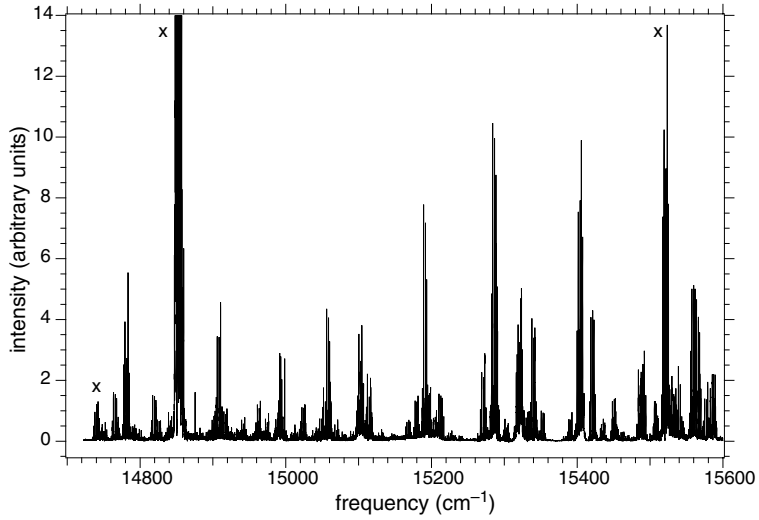

Fig. 2. An overview scan of rotationally resolved vibronic bands in the $A^2B_2 \leftarrow X^2A_1$ transition of $^{15}N^{16}O_2$. The spectra have been recorded with a gated fluorescence setup optimized for low gas consumption and high sensitivity. The three bands marked with X are shown in detail in Figs. 3–5. The strong transition around 14 850 cm^{-1} – that has been clipped here for clarity – is about 3.5 times stronger than the band shown in Fig. 3.

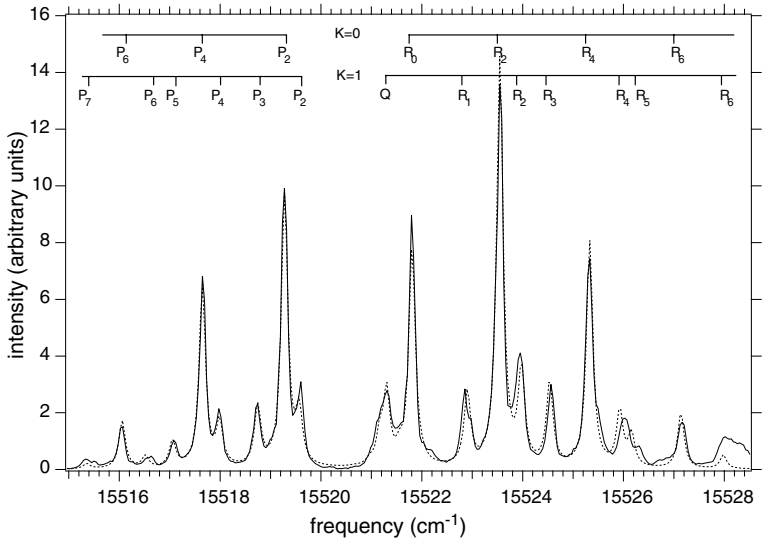

Fig. 3. The rotationally resolved $A^2B_2 \leftarrow X^2A_1$ vibronic band of $^{15}N^{16}O_2$ located at 15520.95(10) cm^{-1}. All transitions are parallel. The five strongest lines belongs to the $K = 0$ stack. The weaker and irregular progression (due to the 'staggering effect') belong to the $K = 1$ stack.

Table 1
Spectroscopic constants of the vibronic bands shown in Figs. 3–5. All values are given in cm^{-1}

Ground state [23]	
A''	7.6308
B''	0.4338
C''	0.40945
14 740 Band	
Origin	14739.8(1)
$(B' + C')/2$	0.424
$\bar{\varepsilon}'$	0.04
14 850 Band	
Origin	14851.3(1)
A'	7.675
B'	0.482
C'	0.444
$\bar{\varepsilon}'$	0.11
15 521 Band	
Origin	15520.95(10)
A'	7.935
B'	0.454
C'	0.400

The fit values are tentative, since they are obtained subject to some restrictions mentioned in the text. The estimated error in the fits of the excited state rotational constants is 0.005 cm^{-1}.

and also centrifugal constants have likewise been neglected.

The possibility of extracting accurate values of the rotational constants in the excited state is important since those values reflect the degree of mixing of the two lowest electronic states and therefore may be helpful in assigning the vibronic band. Unfortunately, the situation is not always that favourable. Then, a complete fit of the spectrum is not worthwhile. Often, the $K = 1$ stack is too weak as to be detectable. Moreover, the fine structure splittings are not normally negligible. As an example, in Fig. 4 another $K = 0$ rovibronic band is shown with a band origin at 14739.8(1) cm^{-1}. The splitting observed for the P_4, P_6 and R_2, R_4 and R_6 transitions is due to spin–rotation interaction in the excited state, as fine structure splitting in the ground state is not resolved with our laser resolution [19]. Including an additional term $\varepsilon'\mathbf{N}\cdot\mathbf{S}$, where $\bar{\varepsilon}' = (\varepsilon'_{bb} - \varepsilon'_{cc})/2$, with $\bar{\varepsilon}'$ indicating the spin rotation coupling tensor and b and c indicating the corresponding inertial axes of NO_2, into a standard fit yields a value $\bar{\varepsilon}' \sim 0.04$ cm^{-1} for the fine structure constant in the excited state. The constants are summarized in Table 1.

One strong and rather isolated band at 14 850 cm^{-1} can be related to an eigenstate having a dominant $A\ ^2B_2$ character. On a larger energy scale high intensity transitions have been reported for $^{14}N^{16}O_2$ in a Fourier Transform Infrared (FTIR) study as a polyad structure [3]. This polyad structure has also been observed by FTIR for the $^{15}N^{16}O_2$ isotopologue by Orphal [20]; the 14851.3 cm^{-1} vibronic energy corresponds to polyad $P = 7$ ($P = 2v_1 + v_2 + v_3$, where v_1, v_2 and v_3 are the quantum numbers for the symmetric, bending and asymmetric vibrations in the excited vibronic state, respectively). The Franck–Condon calculations made for the main isotopologue [3] should remain qualitatively correct for the $^{15}N^{16}O_2$ isotopologue. The vibronic level at 14851.3 cm^{-1} can be assigned a (1,5,0) $^2B_2$ dominant character because of its very strong intensity and its unusually large $\bar{B}' = 0.463$ cm^{-1}. A zoomed figure is shown in Fig. 5, along with a fit spectrum. For clarity, the fits of the $K = 0$ and 1 stacks are also shown separately. The quality of the fit gives the rotational constants in Table 1 with good accuracy, although the fit of

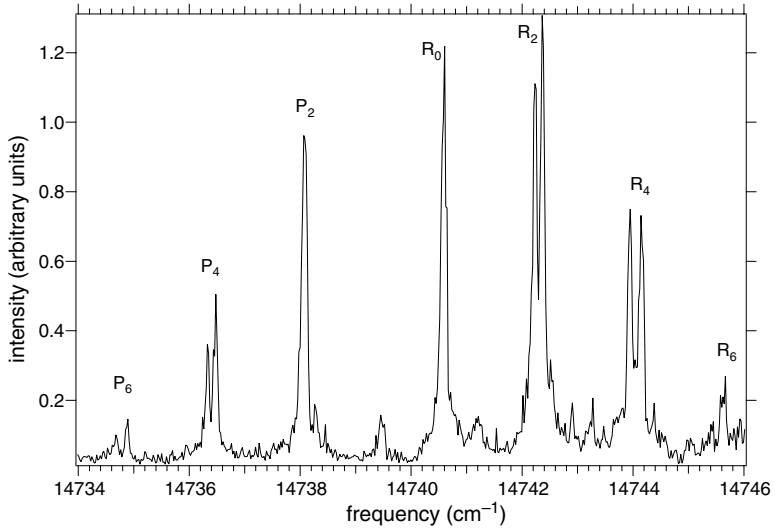

Fig. 4. The rotationally resolved $A^2B_2 \leftarrow X^2A_1$ vibronic band of $^{15}N^{16}O_2$ located at 14739.8(1) cm^{-1}. Only the $K = 0$ stack with resolved fine structure splittings can be observed.

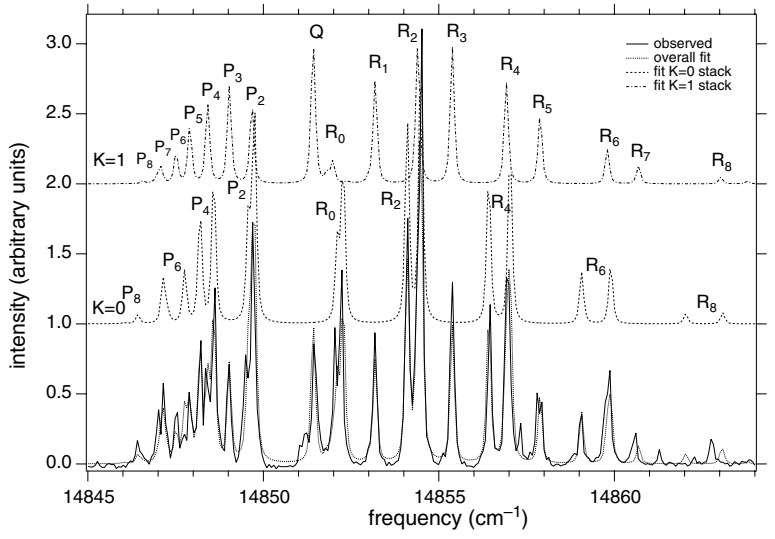

Fig. 5. The rotationally analysed $A^2B_2 \leftarrow X^2A_1$ strong vibronic band of $^{15}N^{16}O_2$ at 14 850 cm^{-1} that is vibrationally assigned to a $(v_1, v_2, v_3) = (1, 5, 0)$ polyad excitation in the excited state. Fits of the $K = 0$ and $K = 1$ stacks are shown separately. Deviations between fitted and observed spectrum do not impede the accuracy of the rotational constants and are related to assumptions regarding the fine structure. The corresponding constants are listed in Table 1.

the fine structure can still be improved. For the $K = 0$ stacks the assumption of a constant $\bar{\varepsilon}' = 0.11$ cm^{-1} for rotational levels up to $N' = 6$ of the excited state is satisfactory, but a clear deviation is visible in the R_8 transition and similarly deviations can be seen in the higher P transitions. There are several possible reasons for those deviations. One reason is the neglect of centrifugal effects, which may not be warranted for N' larger than five or so [21]. Another possible source of deviation is that the spin–rotation coupling constant is actually not constant, but depends on N. In case of strong vibronic coupling the spin–rotation coupling is expected to even have a quadratic dependence on N and this is borne out experimentally (see, e.g. [22]). The fit of the $K = 1$ stack is subject to the same restriction, but here the fine structure splitting may be neglected even if $\bar{\varepsilon}'$ is not negligible. Tentatively, we explain this by assuming that ε'_{aa} increases quadratically with N' and has a negative sign, so that it offsets the effect of $\bar{\varepsilon}'$ and the (positive) value of ε''_{aa} in the ground state. The constants obtained by neglecting the imperfections in the fit, mentioned above, are listed in Table 1. They are of a tentative nature and a more detailed spectral analysis will be given elsewhere. The values of the rotational constants are not, however, expected to significantly change by those refinements.

The strong band at 14 850 cm^{-1} may be particularly useful for detection of $^{15}N^{16}O_2$ and the study of MIF in the atmosphere. In view of the much lower abundances of ^{15}N a strong transition is needed to observe $^{15}N^{16}O_2$ at all. In addition, a comparison with detailed lists of line positions of $^{14}N^{16}O_2$ learns that there is barely an overlap with the strong band discussed here, which makes it very well suited as a benchmark transition.

Special efforts have been made to extend the operation of our setup to lower excitation frequencies, roughly below 13 500 cm^{-1}. As the fluorescence is red shifted with respect to excitation frequency, the PMT is sensitive to only a small part of the total fluorescence signal for laser frequencies roughly above 700 nm. For this reason a LN_2 cooled Ge detector is used that is sensitive also at wavelengths up to 1700 nm [12]. This is of importance as direct information on the (less perturbed) low lying vibrational levels (close to the conical intersection) is required for a fair comparison with theoretical models [1]. Preliminary results indicate that this is an attainable prospective; at a laser excitation wavelength around 700 nm the PMT and Ge detectors give comparable results and from 720 nm onwards the use of the Ge detector results in better S/N ratios.

Acknowledgements

This work has been supported within the Molecular Atmospheric Physics program of the Dutch organisation for fundamental research (FOM). Support by CW (Chemische Wetenschappen) is acknowledged as well. Marijke Koudijzer is thanked for help during the experiments. R.J. belongs to INPG-ENSP Grenoble and thanks the EU for support to access the experimental facilities of the Laser Center Vrije Universiteit through the EU program HPRI-1999-CT-00064.

References

[1] M. Joyeux, R. Jost, M. Lombardi, J. Chem. Phys. 119 (2003) 5923.
[2] R. Jost, M.G. Vergniory, A. Campargue, J. Chem. Phys. 119 (2003) 2590.
[3] J. Orphal, S. Dreher, S. Voigt, J.P. Burrows, R. Jost, A. Delon, J. Chem. Phys. 109 (1998) 10217.
[4] R. Jost, M. Joyeux, M. Jacon, Chem. Phys. 283 (2002) 17.
[5] K. Mauersberger, Geophys. Res. Lett. 8 (1981) 935.
[6] K. Mauersberger, B. Erbacher, D. Krankowsky, J. Günther, R. Nickel, Science 283 (1999) 370.
[7] H. Umemoto, K. Tanaka, S. Oguro, R. Ozeki, M. Ueda, Chem. Phys. Lett. 345 (2001) 44.
[8] Y.Q. Gao, R.A. Marcus, Science 293 (2001) 259.
[9] F. Robert, C. Camy-Peyret, Ann. Geophys. 19 (2001) 229.
[10] C.A. Biesheuvel, J. Bulthuis, M.H.M. Janssen, S. Stolte, J.G. Snijders, J. Chem. Phys. 112 (2000) 3633.
[11] D. Romanini, P. Dupré, R. Jost, Vib. Spectrosc. 19 (1999) 93.
[12] A. Delon, R. Jost, M. Jacon, J. Chem. Phys. 114 (2001) 331.
[13] J. Miyawaki, K. Yamanouchi, S. Tsuchiya, Chem. Phys. Lett. 180 (1991) 287.
[14] Y. Tang, J.P. Schmidt, S.A. Reid, J. Chem. Phys. 110 (1999) 5734.
[15] D. Proch, T. Trickl, Rev. Sci. Instrum. 60 (1989) 713.
[16] J.W. Mellor, A Comprehensive Treatise on Inorganic and Theoretical Chemistry, vol. VIII, Longmans, London, 1962, p. 558.
[17] A. Pedler, F.H. Pollard, in: T. Moeller (Ed.), Inorganic Syntheses, vol. V, McGraw-Hill Book Company, New York, 1957, p. 87.
[18] R. Georges, A. Delon, R. Jost, J. Chem. Phys. 103 (1995) 1732.
[19] W.C. Bowman, F.C. De Lucia, J. Chem. Phys. 77 (1982) 92.
[20] J. Orphal, private communication.
[21] H.J. Vedder, M. Schwartz, H.J. Foth, W. Demtroeder, J. Mol. Spectrosc. 97 (1983) 92.
[22] H.J. Foth, H.J. Vedder, W. Demtroeder, J. Mol. Spectrosc. 88 (1981) 109.
[23] Y. Hamada, J. Mol. Struct. 242 (1991) 367.